

# Identification of Mutations in *Caenorhabditis elegans* That Cause Resistance to High Levels of Dietary Zinc and Analysis Using a Genomewide Map of Single Nucleotide Polymorphisms Scored by Pyrosequencing

Janelle J. Bruinsma,<sup>1</sup> Daniel L. Schneider, Diana E. Davis and Kerry Kornfeld<sup>2</sup>

*Department of Developmental Biology, Washington University School of Medicine, St. Louis, Missouri 63110*

Manuscript received November 9, 2007

Accepted for publication February 20, 2008

## ABSTRACT

Zinc plays many critical roles in biological systems: zinc bound to proteins has structural and catalytic functions, and zinc is proposed to act as a signaling molecule. Because zinc deficiency and excess result in toxicity, animals have evolved sophisticated mechanisms for zinc metabolism and homeostasis. However, these mechanisms remain poorly defined. To identify genes involved in zinc metabolism, we conducted a forward genetic screen for chemically induced mutations that cause *Caenorhabditis elegans* to be resistant to high levels of dietary zinc. Nineteen mutations that confer significant resistance to supplemental dietary zinc were identified. To determine the map positions of these mutations, we developed a genomewide map of single nucleotide polymorphisms (SNPs) that can be scored by the high-throughput method of DNA pyrosequencing. This map was used to determine the approximate chromosomal position of each mutation, and the accuracy of this approach was verified by conducting three-factor mapping experiments with mutations that cause visible phenotypes. This is a generally applicable mapping approach that can be used to position a wide variety of *C. elegans* mutations. The mapping experiments demonstrate that the 19 mutations identify at least three genes that, when mutated, confer resistance to toxicity caused by supplemental dietary zinc. These genes are likely to be involved in zinc metabolism, and the analysis of these genes will provide insights into mechanisms of excess zinc toxicity.

**M**ETALS such as zinc, iron, and copper play essential roles in biological systems. Here we focus on zinc, since it is one of the most abundant metals in animals and it has a wide range of functions. Zinc is a divalent cation that is not redox active in biological systems. Zinc is an essential catalytic component of >300 enzymes (in all six major classes) and a critical component of structural motifs such as zinc fingers (VALLEE and FALCHUK 1993). The analyses of several eukaryotic genomes have led to the estimate that zinc may be required for the function of >3% of all proteins (LANDER *et al.* 2001). Zinc has also been implicated in signaling processes and may be a signaling molecule: zinc is concentrated in some synaptic vesicles and then released into the synapse where it might modulate neurotransmission (FREDERICKSON and BUSH 2001; COLVIN *et al.* 2003; WALL 2005; YAMASAKI *et al.* 2007). Zinc affects epidermal growth factor receptor/Ras-mediated signal transduction, thus playing a role in cell fate determination (WU *et al.* 1999; BRUINSMA *et al.* 2002; SAMET *et al.* 2003; YODER *et al.* 2004). The importance of the processes that involve

zinc is demonstrated by the observation that severe zinc deficiency is incompatible with growth and survival. Although zinc is essential, excess zinc can be deleterious. The mechanisms of excess zinc toxicity have not been well defined, but a plausible model is that excess zinc binds inappropriate sites in proteins or cofactors, perhaps replacing the physiologically relevant metals (ZHAO and EIDE 1997).

Because zinc is essential but also potentially toxic, organisms must have systems for efficient zinc uptake and distribution but also systems for zinc excretion or detoxification. These systems must involve mechanisms that sense zinc levels and trigger a regulatory response to achieve zinc homeostasis (TAPIERO and TEW 2003). Important progress has been made in characterizing proteins involved in zinc metabolism and mechanisms of zinc homeostasis. However, the understanding of these processes remains incomplete. The best-characterized model systems of zinc metabolism and homeostasis are single-celled organisms, such as bacteria and yeast (reviewed by GAITHER and EIDE 2001; EIDE 2003; HANTKE 2005). Some mechanisms of zinc metabolism defined in yeast appear to be conserved in vertebrates (LIUZZI and COUSINS 2004). Because zinc is a hydrophilic ion that cannot diffuse passively across membranes, specific transport mechanisms are required for it to enter and exit cells and organisms. Two major

<sup>1</sup>Present address: EMD Chemicals, Madison, WI 53719.

<sup>2</sup>Corresponding author: Department of Developmental Biology, Washington University School of Medicine, Campus Box 8103, 660 S. Euclid Ave., St. Louis, MO 63110. E-mail: kornfeld@wustl.edu

families of zinc transporters have been characterized. The Zrt-, Irt-like protein (ZIP) family of proteins (a.k.a. SLC39) functions to increase cytosolic zinc levels by importing zinc either across the plasma membrane or across the membrane of intracellular organelles (reviewed by ENG *et al.* 1998; GUERINOT 2000; EIDE 2004). The cation diffusion facilitator (CDF) family of proteins (a.k.a. SLC30) functions to decrease cytosolic zinc levels by exporting zinc either across the plasma membrane or across the membrane of intracellular organelles (reviewed by PALMITER and HUANG 2004). Vertebrate genomes encode many predicted CDF and ZIP proteins, and several have been demonstrated to influence zinc metabolism in animals: the human protein Zip4 is defective in patients with acrodermatitis enteropathica (KURY *et al.* 2002; WANG *et al.* 2002), the mouse CDF protein ZnT-4 is affected in *lethal milk* mutants (HUANG and GITSCHIER 1997), the human CDF protein ZnT-8 is highly expressed in pancreatic islet cells that secrete insulin, and a polymorphism in the ZnT-8 gene has been demonstrated to be a risk factor for type 2 diabetes in humans (CHIMIANTI *et al.* 2006; SLADEK *et al.* 2007).

Members of the ZIP and CDF protein families are regulated at multiple levels to promote zinc homeostasis. Several genes involved in zinc metabolism have been shown to display changes in gene transcription in response to changes in environmental zinc. These transcriptional changes are mediated by zinc-sensitive transcription factors (ZHAO *et al.* 1998; BIRD *et al.* 2000). In higher eukaryotes, metal-regulatory transcription factor-1 (MTF-1) binds to metal responsive elements (MREs) in promoters of genes involved in zinc metabolism (*e.g.*, *Znt1*; reviewed by LICHTLEN and SCHAFFNER 2001). Furthermore, post-translational regulation is important for ZIP proteins in yeast (GITAN and EIDE 2000).

An important process that is not well characterized is the response of animals to excess zinc, including the roles of excretion and storage. Studies of yeast suggest that excess zinc is not excreted across the plasma membrane but rather is stored in the vacuole. Storage systems in multicellular animals have not been well defined. The metallothionein family of proteins has been proposed to play roles in zinc metabolism and/or detoxification (COYLE *et al.* 2002; VASAK 2005). Metallothioneins are small, cysteine-rich proteins with the capacity to bind up to seven zinc atoms per protein. Metallothionein genes contain MREs in the promoters that are bound by MTF-1. Thus, the transcription of metallothionein genes is regulated by zinc levels. Metallothioneins may function to store or detoxify zinc and thus contribute to the capacity of the animals to tolerate high levels of zinc (MARET 2003).

The free-living soil nematode *Caenorhabditis elegans* has been utilized extensively for studies of development and neurobiology, and sophisticated genetic and molecular approaches are well established (RIDDLE *et al.*

1997). The *C. elegans* system has great potential for investigating mechanisms of zinc metabolism in an intact animal, although studies conducted thus far have been limited. The completely sequenced *C. elegans* genome encodes predicted proteins with similarity to zinc transporters, including 14 ZIP proteins and 13 CDF proteins (GAITHER and EIDE 2001; K. ANANTH and K. KORNFELD, unpublished observations). Two genes that encode members of the CDF family have been demonstrated to play a role in zinc metabolism: *cdf-1* and *sur-7*. *cdf-1(lf)* and *sur-7(lf)* mutants display dose-dependent developmental delays when cultured on standard nematode growth media supplemented with zinc, indicating that these genes are necessary for zinc tolerance (BRUINSMA *et al.* 2002, YODER *et al.* 2004). Mutations of both genes were identified in genetic screens for mutants with abnormal vulval formation, and both genes play a role in Ras-mediated signaling during vulval development. The functions of CDF-1 and SUR-7 in zinc metabolism were characterized secondarily, after it was appreciated that the predicted proteins were members of the CDF family. *C. elegans* contains two metallothionein genes, *mtl-1* and *mtl-2*. The transcription of these genes is induced by cadmium exposure and other stresses that do not involve metals, but not by high levels of zinc exposure. Loss-of-function mutants of *mtl-1* and *mtl-2* display enhanced cadmium toxicity, but a role in zinc metabolism has not been detected (FREEDMAN *et al.* 1993; MOILANEN *et al.* 1999; SWAIN *et al.* 2004). Phytochelatins are peptides that can bind metals and contribute to cadmium tolerance. *C. elegans pcs-1* mutants (defective in phytochelatin synthesis) and *hmt-1* mutants (defective in phytochelatin transport) display enhanced cadmium toxicity (VATAMANIUK *et al.* 2001, 2005). These results indicate that metallothioneins and phytochelatins are involved in cadmium detoxification. *C. elegans* genes that have been shown to play a role in the metabolism of zinc or other metals were identified by either (1) candidate approaches based on the involvement of similar proteins in metal biology in other organisms or (2) genetic screens for vulval defective mutants. It is likely that many genes involved in zinc metabolism remain uncharacterized, since genetic screens for mutants that are abnormal in the metabolism of zinc or other metals have not been reported.

To exploit *C. elegans* to investigate mechanisms of zinc metabolism in a multicellular organism, we conducted a forward genetic screen for mutations that promote resistance to the toxicity caused by supplemental dietary zinc. This approach is relatively unbiased, since it relies on a random chemical mutagenesis and a direct assay of zinc metabolism. To conduct this analysis, we first developed culture conditions that permit supplementation with zinc and characterized the dose-dependent response of wild-type worms to supplemental dietary zinc. We conducted a large-scale screen and identified 19 zinc-resistant mutants. A critical aspect of forward

genetic screens is positioning the mutations in the genome. Single nucleotide polymorphism (SNP) markers have several advantages for mapping, and genome-wide maps of SNP markers that rely on specific methods to score the SNPs have been described for *C. elegans* (WICKS *et al.* 2001; SWAN *et al.* 2002; DAVIS *et al.* 2005; ZIPPERLEN *et al.* 2005; SHELTON 2006). To position the new mutations in the *C. elegans* genome, we developed a genome-wide map of SNP markers that can be scored by the high-throughput method of pyrosequencing, a scoring method not previously described for genome-wide SNP maps in *C. elegans*. This map was used to determine the approximate chromosomal position of each mutation, and the accuracy of this approach was verified by conducting three-factor mapping experiments with mutations that cause visible phenotypes. This map of SNP markers is likely to be generally useful for mapping mutations in *C. elegans*. The mapping experiments demonstrate that the 19 mutations identify at least three genes that, when mutated, confer resistance to toxicity caused by supplemental dietary zinc. These results demonstrate the feasibility of directly screening for mutants with abnormal zinc metabolism and document a new phenotype for *C. elegans* mutants: resistance to excess zinc toxicity. The genes affected by these mutations are likely to play important roles in zinc metabolism.

## MATERIALS AND METHODS

**General methods and strains:** *C. elegans* strains were cultured as described by BRENNER (1974) and grown at 20° unless otherwise noted. The wild-type strain and parent of all mutant strains was N2, a wild-type isolate from Bristol, United Kingdom. CB4856 is a wild-type isolate from Hawaii used for SNP mapping. The following mutations that cause a visible phenotype and were used to mark chromosomes are described by RIDDLE *et al.* (1997): LGI—*lin-17(n671)*, *sup-11(n403)*, *unc-11(e47)*, and *dpy-5(e61)*; LGV—*unc-46(e408)*, *dpy-11(e224)*, and *unc-42(e270)*; LGX—*lon-2(e678)*, *unc-6(n102)*, *dpy-6(e14)*, *unc-115(e2225)*, *egl-15(n484)*, *sma-5(n678)*, and *unc-9(e101)*. *cdf-1(n2527)* was described by JAKUBOWSKI and KORNFELD (1999).

**Culturing *C. elegans* on Noble agar minimal media:** To make Noble agar minimal media (NAMM), we prepared a solution with 1.7% Noble agar (U. S. Biological, Swampscott, MA) and a final concentration of 5 mg/liter cholesterol using a stock solution of 5 mg/ml cholesterol in 100% ethanol using water from a Milli-Q synthesis A10 machine [UV photo-oxidation purification system that decreases zinc levels to the range of parts per billion (Millipore, Billerica, MA)]. The solution was autoclaved and cooled to 50°, and 7 ml was dispensed into each 6-cm petri dish. To supplement NAMM with zinc, we added 1 M zinc sulfate solution [ $ZnSO_4 \cdot 7H_2O$  (Sigma, St. Louis)] made with autoclaved Milli-Q water to the molten, autoclaved NAMM to obtain the desired final zinc concentration and then dispensed this into petri dishes. The media were allowed to solidify at room temperature overnight, and the dishes were used immediately or stored at 4°. We typically used dishes within 1 week of preparation, since long-term storage might result in evaporative loss that could affect the concentration of zinc in the NAMM.

NAMM does not support bacterial growth. To provide bacteria as a food source for the worms, we grew *Escherichia coli* OP50 overnight in LB, pelleted the bacteria by centrifugation, resuspended the pelleted bacteria in 1/10 initial volume with Milli-Q water sterilized by autoclaving, and dispensed 50–100  $\mu$ l/petri dish. The dishes were gently swirled to distribute bacteria in a thin layer. After several hours, the excess liquid was absorbed and the petri dish was ready for use. To introduce worms onto NAMM dishes, we typically (1) picked eggs from nematode growth media (NGM) dishes with a platinum wire or (2) treated adult hermaphrodites grown on NGM with alkaline hypochlorite solution to purify eggs, washed the eggs with M9 buffer, and dispensed the eggs onto NAMM dishes by pipetting.

**Isolation of zinc-resistant mutants:** To isolate zinc-resistant mutants, we mutagenized N2 hermaphrodites with ethyl methanesulfonate (EMS) as described in BRENNER (1974), *N*-ethyl-*N*-nitrosourea (ENU) as described by DE STASIO *et al.* (1997), or UV-activated trimethyl psoralen (UV/TMP) (YANDELL *et al.* 1994) as described in GOLDSTEIN *et al.* (2006). We picked mutagenized N2 hermaphrodites at the L4 larval stage and allowed these animals to self-fertilize on NGM dishes. F<sub>1</sub> self-progeny, adult hermaphrodites were treated with alkaline hypochlorite solution, and F<sub>2</sub> eggs were isolated. These F<sub>2</sub> eggs were dispensed onto NAMM + 0.3 mM ZnSO<sub>4</sub> dishes. Dishes were screened for viable F<sub>2</sub> animals that had matured to a late larval stage or adulthood after 4–7 days. F<sub>2</sub> animals that met this criteria were picked individually to standard NGM dishes and allowed to self-fertilize to establish a population. To estimate the frequency of false positives, we analyzed unmutagenized N2 animals in parallel. These dishes typically displayed no late larval stage or adult animals, indicating that the rate of false positives was very low.

To determine if the candidate strain displayed a high penetrance zinc-resistance phenotype, we tested 500–1000 eggs for the ability to mature to the late larval or adult stage in 4–7 days on NAMM + 0.3 mM ZnSO<sub>4</sub>. Our minimum criteria for continued analysis was that the strain displayed a survival penetrance of at least 10%. Using EMS mutagenesis, we screened ~92,600 haploid genomes and picked 47 candidate mutants of which 9 (19%) met the criteria for further analysis; these included *am118*, *am120*, *am128*, *am129*, and *am130*, which were backcrossed, and four mutations that were not backcrossed successfully. Using ENU mutagenesis, we screened ~77,900 haploid genomes and picked 59 candidate mutants of which 13 (22%) met the criteria for further analysis, including *am122*, *am123*, *am124*, *am125*, *am126*, *am132*, *am133*, *am134*, *am136*, *am137*, *am138*, *am139*, and *am140*. Using UV/TMP mutagenesis, we screened ~132,900 haploid genomes and picked three candidate mutants of which one (33%) met the criteria for further analysis (*am135*). Each of these 19 mutant strains was backcrossed to wild-type N2 at least twice using standard methods by scoring the phenotype of resistance to 0.3 mM supplemental zinc in NAMM.

**Mapping mutations relative to SNP markers in CB4856:** To determine the linkage relationships of mutations that cause zinc resistance and SNP markers in CB4856, we mated mutant males to CB4856 hermaphrodites and placed hermaphrodite cross-progeny on separate petri dishes. When these hermaphrodites matured to the gravid adult stage, we isolated F<sub>2</sub> eggs by treatment with alkaline hypochlorite solution. Eggs were deposited on NAMM + 0.3 mM ZnSO<sub>4</sub> dishes. To isolate homozygous mutants, we picked F<sub>2</sub> hermaphrodites that had matured to the late larval or adult stage. These hermaphrodites were propagated by self-fertilization for about five generations on NGM so that most loci would become homozygous. These populations were retested to confirm the zinc-resistance phe-

notype and were used to prepare genomic DNA according to the method of WILLIAMS *et al.* (1992).

To identify SNPs in the CB4856 strain, we used the database described by WICKS *et al.* (2001) that contains many candidate SNPs identified by sequencing randomly generated fragments of DNA. We used the software supplied by the manufacturer [Biotage, Charlottesville, VA (formerly Pyrosequencing)] to design amplification and sequencing primers, and we selected candidate SNPs where the primers were predicted to have a high probability of success. In these cases, the pyrosequencing assay was almost always successful. Pyrosequencing reactions were performed according to the manufacturer's instructions (<http://www.pyrosequencing.com>). Briefly, in a 96-well plate, one biotinylated amplification primer and one standard amplification primer were used to PCR amplify the region containing a SNP, a step that requires ~2 hr. The single-stranded product was vacuum purified using streptavidin sepharose (GE Healthcare, Piscataway, NJ), the sequencing primer was added, the sequencing reaction was performed using model PSQ 96 MA (Biotage), and the data were analyzed using software supplied by the manufacturer. These steps required <1 hr. The manufacturer's estimated cost for reagents is \$0.80/reaction. The total cost per reaction also includes the cost of labor to process the samples (several hours per 96-well plate) and a fraction of the purchase and maintenance cost of the instrument.

**Three-factor mapping experiments:** We used standard methods to conduct three-factor mapping experiments (BRENNER 1974). The following results were obtained with *am120* on chromosome I using genes with the following map positions: *lin-17*, -7.43; *sup-11*, -5.71; *unc-11*, -2.52; and *dpy-5*, 0.00. From *am120/lin-17 sup-11* hermaphrodites, 2/2 Lin non-Sup self-progeny segregated *am120*. From *am120/lin-17 unc-11* hermaphrodites, 3/4 Lin non-Unc self-progeny segregated *am120*. From *am120/sup-11 dpy-5* hermaphrodites, 5/11 Dpy non-Sup self-progeny segregated *am120*. These results indicate that *am120* is positioned right of *lin-17* and left of *unc-11* and *dpy-5*.

The following results were obtained with *am132* on chromosome X using genes with the following map positions: *lon-2*, -6.74; *unc-6*, -2.01; *dpy-6*, 0.00; *unc-115*, +1.88; *egl-15*, +2.86; *sma-5*, +7.01; and *unc-9*, +10.25. From *am132/lon-2 unc-6* hermaphrodites, 12/13 Lon non-Unc and 0/5 Unc non-Lon self-progeny segregated *am132*. From *am132/dpy-6 unc-9* hermaphrodites, 5/12 Dpy non-Unc self-progeny segregated *am132*. From *am132/egl-15 sma-5* hermaphrodites, 0/11 Egl non-Sma self-progeny segregated *am132*. From *am132/egl-15 unc-115* hermaphrodites, 2/9 Egl non-Unc self-progeny segregated *am132*. These results indicate that *am132* is positioned right of *lon-2*, *unc-6*, *dpy-6*, and *unc-115* and left of *egl-15*, *sma-5*, and *unc-9*.

The following results were obtained with *am138* on chromosome V using genes with the following map positions: *unc-46*, -2.49; *dpy-11*, 0.00; and *unc-42*, +2.16. Because mutations that are positioned near *am138* and cause a visible phenotype influenced zinc resistance, we selected self-progeny that displayed a zinc-resistance phenotype and then analyzed the segregation of recessive visible markers. From *am138/unc-46 dpy-11* hermaphrodites, we analyzed 63 zinc-resistant self-progeny: 40 failed to segregate Unc, Dpy, or Unc Dpy; 21 segregated Unc Dpy; and 2 segregated Unc non-Dpy. These results indicate that *am138* is positioned to the right of *unc-46* and *dpy-11*. From *am138/dpy-11 unc-42* hermaphrodites, we analyzed 75 zinc-resistant self-progeny: 43 failed to segregate Unc, Dpy, or Unc Dpy; 27 segregated Unc Dpy; 3 segregated Dpy non-Unc; and 2 segregated Unc non-Dpy. These results indicate that *am138* is positioned between *dpy-11* and *unc-42*. We interpret zinc-resistant self-progeny that segregate Unc

Dpy progeny as heterozygous for the semidominant *am138* mutation and thus not informative for mapping.

## RESULTS

### Establishing culture conditions for dietary zinc supplementation—growth and development of wild-type worms can be impaired by supplemental dietary zinc:

To effectively use *C. elegans* as a model system to analyze zinc metabolism, we first developed methods to manipulate dietary zinc. The standard culture conditions for *C. elegans* established by BRENNER (1974) involve culturing worms on an agar surface in a petri dish, since the worms can be easily visualized and manipulated. The NGM agar contains peptone, salt, cholesterol, and agar that support the growth of a lawn of *E. coli* and the worms eat the *E. coli*. Regarding zinc, *E. coli* obtains zinc from the NGM. The worms are likely to obtain zinc primarily from ingested *E. coli*, but worms may also obtain zinc from ingested media. The precise amount of zinc obtained by worms grown in NGM with live *E. coli* has not been defined. To increase the amount of zinc ingested by the worms, we previously added supplemental zinc to NGM agar (BRUINSMA *et al.* 2002). In these growth conditions, the worms are likely to ingest more zinc because the concentration of zinc in the bacteria is increased and/or the concentration of zinc in the directly ingested media is higher. The addition of 2 mM ZnSO<sub>4</sub> to NGM significantly impaired the growth and development of *cdf-1(n2527)* mutants, but it had no significant effect on the growth and development of wild-type worms (BRUINSMA *et al.* 2002). Similarly, YODER *et al.* (2004) demonstrated that adding supplemental zinc to NGM affected *sur-7(ku119)* mutants but did not affect wild-type worms significantly. However, while performing these experiments, we noted that the supplemental zinc was prone to form visible precipitates at concentrations >1 mM. These studies suggest that supplemental zinc added to NGM media does result in increased zinc intake by worms, since it affected *cdf-1* and *sur-7* mutant worms. However, the amount of additional ingested zinc was not large enough to affect wild-type worms, and the solubility limits of supplemental zinc in NGM prevented this system from being useful for defining the response of wild-type worms to supplemental dietary zinc.

To address the problem of limited zinc solubility, we analyzed the solubility of zinc in each component of NGM. Zinc salts were relatively insoluble in standard grade agar and potassium phosphate solutions, whereas zinc salts were highly soluble in the other ingredients of NGM (data not shown). To address the zinc-sulfate solubility limits in standard-grade agar, we analyzed a highly purified agar, called Noble agar (U. S. Biological). Zinc sulfate was soluble to ~8 mM in 1.7% Noble agar (data not shown). Since zinc phosphates have very low solubility in aqueous solutions, we decided to

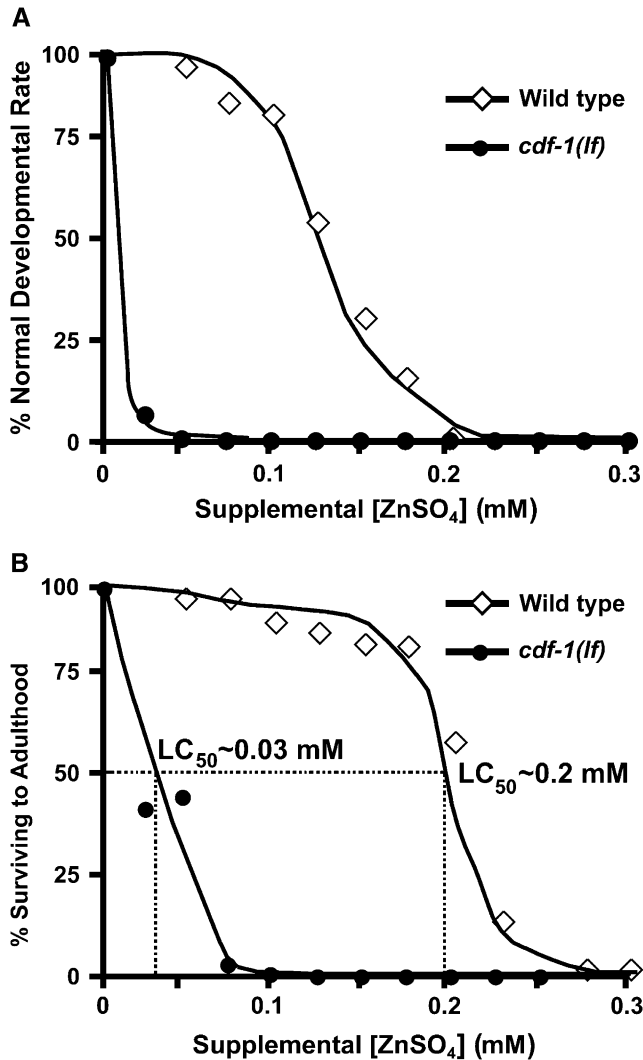


FIGURE 1.—Supplemental dietary zinc caused dose-dependent development delays and lethality. Wild-type animals (open diamonds) and *cdf-1(n2527)* mutants (solid circles) were cultured on NAMM with supplemental zinc sulfate starting at the egg stage, and development was monitored daily. (A) Animals that did not progress to the adult stage within 4 days were defined as not displaying a normal developmental rate. Each data point represents  $\sim 100$  animals. (B) Animals that did not progress to the adult stage within 10 days were defined as not surviving to adulthood. Most animals that did not survive to adulthood died as L1 larvae. The concentration of supplemental zinc that caused  $\sim 50\%$  lethality ( $LC_{50}$ ) is indicated.

remove potassium phosphate. We also removed the other components that support bacterial growth and named this new media “Noble agar minimal medium” (NAMM). NAMM consists of 1.7% Noble agar and cholesterol, and it does not support bacterial growth. To provide a food source for worms cultured on NAMM, we grew *E. coli* OP50 in liquid LB media, concentrated the bacteria 10-fold, and aliquoted the live bacteria onto the NAMM. Worms cultured in these conditions displayed a developmental rate and morphology that are

similar to worms cultured on NGM with live *E. coli* (data not shown).

To characterize the response of wild-type worms to supplemental dietary zinc, we analyzed the growth and survival of wild-type worms on NAMM using a wide range of concentrations of supplemental zinc in the form of ZnSO<sub>4</sub>. Wild-type animals cultured in NAMM progress from the egg stage to the adult stage within 4 days at 20°. We defined a developmental delay as animals that developed from the egg stage to the adult stage in  $>4$  days at 20°. Figure 1A shows that supplemental dietary zinc caused a dose-dependent developmental delay: in the absence of supplemental zinc,  $\sim 100\%$  of animals develop at a normal rate, and this fraction decreases to 0% at 0.2 mM supplemental zinc. Animals that displayed a developmental delay frequently had a prolonged L1 larval phase (data not shown). After animals progressed through the L1 stage, development typically proceeded at a normal rate. In addition to the dose-dependent increase in penetrance, measured as the fraction of animals that display a developmental delay, we also observed a dose-dependent increase in expressivity, measured as the duration of the delay. At higher concentrations of supplemental zinc, a significant number of wild-type animals arrested as L1 larvae. The concentration of supplemental zinc that resulted in 50% of wild-type animals arresting as L1 larvae ( $LC_{50}$ ) was  $\sim 0.2$  mM, and the  $LC_{100}$  was  $\sim 0.3$  mM (Figure 1B). Previous studies of zinc supplementation in NGM did not demonstrate a lethal effect in wild-type animals (BRUINSMAN *et al.* 2002), but the amount of zinc available to the worms was limited by zinc solubility. These results with NAMM demonstrate that high levels of zinc are indeed toxic to wild-type worms.

We utilized the NAMM media to characterize the effects of supplemental zinc on *cdf-1(n2527)* mutants. Compared to wild-type animals, *cdf-1* mutants are hypersensitive to supplemental zinc. The mutants displayed a highly penetrant developmental delay when cultured with 0.025 mM supplemental zinc, whereas wild-type animals were not affected significantly by this concentration of supplemental zinc (Figure 1A). The  $LC_{50}$  for *cdf-1(n2527)* mutants was  $\sim 0.03$  mM, nearly sevenfold lower than the  $LC_{50}$  for wild-type animals (Figure 1B).

**A forward genetic screen to identify mutants resistant to supplemental dietary zinc:** Genetic screens have been effective in dissecting a wide range of biological processes in *C. elegans*. To use this approach to characterize zinc metabolism, we took advantage of the NAMM media by screening for mutants that are resistant to the growth arrest caused by supplemental zinc. We mutagenized P<sub>0</sub> wild-type hermaphrodites with EMS, ENU, or UV/TMP at the L4 stage, allowed mutagenized P<sub>0</sub> hermaphrodites to self-fertilize on NGM to generate F<sub>1</sub> progeny, collected F<sub>2</sub> eggs, and deposited F<sub>2</sub> eggs on NAMM supplemented with 0.3 mM

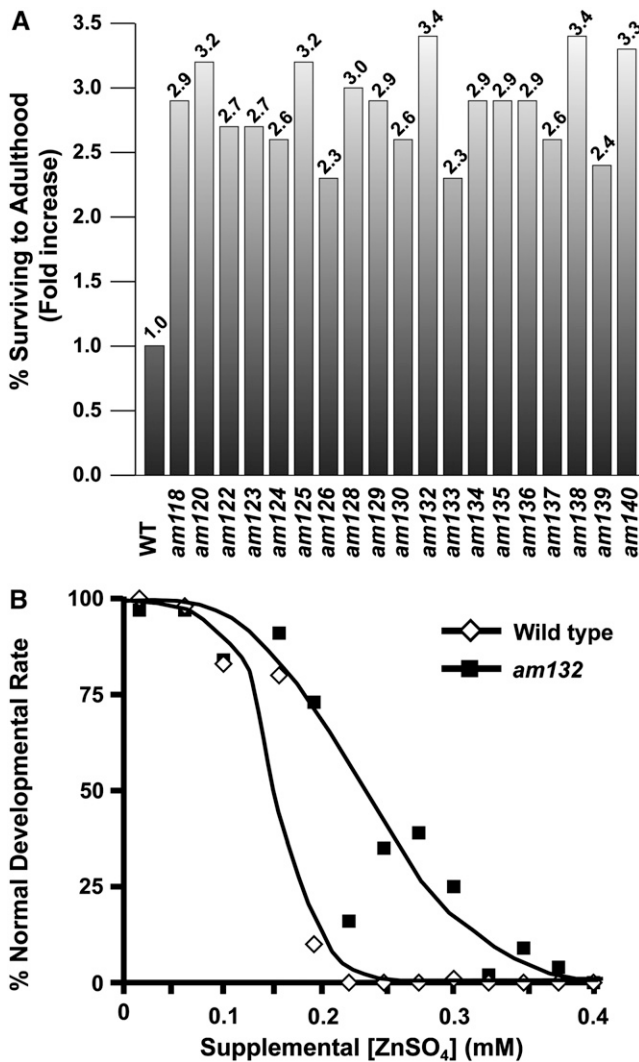


FIGURE 2.—Phenotypic analysis of zinc-resistant mutants. (A) For wild-type and mutant strains (designated *am118*–*am140*), ~100 eggs were placed individually on petri dishes and development was monitored for 10 days. About 25% of wild-type animals matured to adulthood in this time, and mutant values were normalized by setting the wild-type value to 1.0. (B) Wild-type animals (open diamonds) and *am132* mutants (solid squares) were cultured on NAMM with supplemental zinc sulfate starting at the egg stage, and development was monitored daily. Animals that did not progress to the adult stage within 4 days were defined as not displaying a normal developmental rate. Each data point represents ~100 animals.

zinc sulfate. A fraction of the F<sub>2</sub> animals will be homozygous for newly induced mutations. Since 0.3 mM supplemental zinc caused almost 100% of wild-type animals to arrest as L1 larvae, we reasoned that animals that developed to the adult stage in these media conditions are likely to have a newly induced mutation affecting a gene involved in zinc metabolism.

We selected individual animals that developed on NAMM with 0.3 mM supplemental zinc, cultured these animals on NGM to establish a population, and tested

these populations for resistance to 0.3 mM supplemental zinc in NAMM. To gain statistical power, we typically tested >1000 eggs from these populations. If > ~10% of the animals developed to adults in 0.3 mM supplemental zinc, then the strain was scored as retesting positive and pursued further. We analyzed a total of ~300,000 mutagenized genomes and identified 23 strains that retested as zinc resistant (9 EMS, 13 ENU, and 1 UV/TMP).

**Phenotypic characterization of zinc-resistant mutants:** To eliminate extraneous mutations, we backcrossed each strain to wild-type animals. We crossed wild-type males to P<sub>0</sub> mutant hermaphrodites, selected outcrossed F<sub>1</sub> hermaphrodites, established populations from F<sub>2</sub> hermaphrodites, and deposited F<sub>3</sub> eggs on NAMM supplemented with 0.3 mM zinc sulfate. Populations that displayed resistance to supplemental zinc were considered backcrossed. We successfully backcrossed 19 of the 23 strains, and each of these 19 strains was backcrossed twice. These studies indicate that each of these 19 strains contains a single mutation that causes the zinc-resistance phenotype.

The phenotype of survival in NAMM supplemented with 0.3 mM zinc was useful for the isolation and backcrossing experiments because there is essentially no background of surviving wild-type animals. To characterize the performance of these mutants in a less extreme zinc environment and assess zinc resistance quantitatively, we analyzed survival using NAMM supplemented with a lower concentration of zinc. NAMM supplemented with 0.22 mM zinc was used because this zinc concentration results in ~25% survival of wild-type animals, making it possible to quantitatively compare zinc-resistant mutants to wild type. We analyzed ~100 eggs, 1 per petri dish, by monitoring the developing animal for 10 days and scoring adult animals. For the 19 mutant strains, the percentage of survival to adulthood varied from 63 to 92%; in each case, mutant survival was significantly greater than wild-type survival ( $P < 0.005$ , Fisher's exact test). Figure 2A shows the fold increase in survival for each mutant compared to wild type; the fold increase varied from 2.3 to 3.4. These studies demonstrate that the mutant strains are resistant to two different concentrations of supplemental zinc, suggesting that the survival curve with increasing concentrations of supplemental zinc is shifted to the right for each mutant strain.

To characterize the response of a mutant to varying concentrations of supplemental zinc, we analyzed the *am132* mutant strain using 13 concentrations of supplemental zinc. The rate of development was monitored, and we defined normal as the ability to form an adult in ≤4 days. At the lowest concentrations of supplemental zinc, nearly 100% of *am132* mutants developed at a normal rate, and the mutants were not significantly different from wild type (Figure 2B). *am132* mutant worms were more resistant to supplemental zinc than

wild-type animals at concentrations from 0.2 mM to 0.35 mM. At higher concentrations, nearly 100% of the *am132* mutants and wild-type animals developed abnormally. This comprehensive analysis demonstrates that the zinc-resistance curve is shifted to the right for the *am132* mutant strain.

To determine if the newly identified mutations cause phenotypes in standard culture conditions, we examined these strains in the absence of supplemental zinc for phenotypes such as morphological abnormalities, uncoordinated movement, defective male mating, reduced brood size, or delayed developmental rates. All of the strains appeared to be healthy and fertile, and no obvious abnormalities were observed.

**Development of a genome-wide map of SNPs that can be scored by DNA pyrosequencing:** To characterize the zinc-resistant mutants, we decided to map the mutations to a position in the genome. This would provide valuable information because it indicates how many genes are affected by this collection of mutations and facilitates molecular identification of these genes. We decided to use SNP markers to map the mutations for several reasons. Compared to mutations that cause a visible phenotype, SNP markers have the advantage for mapping experiments that they may not cause a phenotype that affects zinc resistance. Furthermore, the strain CB4856 contains thousands of SNPs distributed throughout the genome compared to the standard laboratory strain N2, many of which have been identified (WICKS *et al.* 2001). This makes it possible to map a newly identified mutation relative to many different SNP markers with a single cross.

Although SNP markers have been used extensively to map *C. elegans* genes, a limitation of several of these studies is that the SNP markers were scored by methods that are not amenable to high-throughput scoring, such as DNA sequencing or restriction enzyme digests followed by gel electrophoresis (JAKUBOWSKI and KORNFIELD 1999; WICKS *et al.* 2001; DAVIS *et al.* 2005). High-throughput methods to score *C. elegans* SNPs or small insertion/deletion polymorphisms have been described on the basis of fluorescence polarization-template-directed incorporation (FP-TDI) (SWAN *et al.* 2002), fragment length polymorphism (FLP) assays using a capillary sequencer (ZIPPERLEN *et al.* 2005), and fluorescence-based quantitative PCR (SHELTON 2006). Each of these scoring methods requires specialized equipment.

We chose to use the method of pyrosequencing because it allows high-throughput scoring of SNPs and the technology is affordable for an individual laboratory (reviewed by RONAGHI 2001; FAKHRAI-RAD *et al.* 2002; LANGAEE and RONAGHI 2005; AHMADIAN *et al.* 2006). Briefly, the pyrosequencing method involves three steps. First, the region containing the SNP is PCR amplified using one biotinylated oligonucleotide primer and one standard oligonucleotide primer, and the single-stranded amplified product is affinity purified using

streptavidin. Second, a sequencing primer is annealed to the amplified, single-stranded product adjacent to the position of the polymorphism. Third, nucleotides are added one at a time, and complementary nucleotides are incorporated into the sequencing primer by DNA polymerase. The pyrophosphate that is released upon incorporation of the nucleotide is converted into light by a series of enzymatic reactions, and the light is detected by the Pyrosequencer. The amount of light emitted is proportional to the number of nucleotides incorporated, so that the method provides a quantitative assessment of nucleotide incorporation. This method allows the determination of a short stretch of DNA sequence. Pyrosequencing is conducted in 96-well plates and does not require gel electrophoresis, so that it is possible to rapidly analyze large numbers of samples. Figure 3 shows two examples of using pyrosequencing to analyze *C. elegans* SNPs. These results demonstrate that the method is quantitative and can be used to readily distinguish homozygous from heterozygous animals.

To create a genome-wide map of SNP markers that can be scored by pyrosequencing, we selected five to eight SNPs per chromosome that were well suited to detection by the pyrosequencing method. These SNPs were selected from verified and predicted SNPs identified by randomly sequencing CB4856 DNA (WICKS *et al.* 2001). We designed and verified two oligonucleotide primers that amplify the region containing each SNP and one oligonucleotide primer that sequences the polymorphic site for each SNP (Figure 3 and data not shown). Table 1 provides the name of each SNP, the location in the genome, the nucleotide substitution in the CB4856 strain, and the three oligonucleotide primers that were used to analyze the SNP. Figure 4 shows the position of each SNP marker on the genetic map of *C. elegans*. These markers are well distributed throughout the genome, including markers positioned on the arms of each chromosome and clusters of markers positioned near the center of each chromosome.

**Positioning mutations that cause zinc resistance on the genetic map using SNP markers:** To use the SNP markers to position the zinc-resistant mutations on the genetic map, we first analyzed the zinc resistance of the CB4856 strain. If the CB4856 strain displayed resistance to supplemental zinc that was significantly higher than the N2 strain that was used to generate and backcross the mutations, then it might be difficult to score the zinc-resistance phenotype caused by these mutations in a mixed N2 and CB4856 background. CB4856 hermaphrodites displayed sensitivity to supplemental zinc that was similar to N2 hermaphrodites (data not shown). Specifically, CB4856 hermaphrodites cultured in NAMM supplemented with 0.3 mM zinc displayed ~100% L1 larval lethality. These findings suggest that the zinc-resistance phenotype caused by the newly identified mutations can be scored in a mixed N2 and CB4856 background. Although both starting strains are

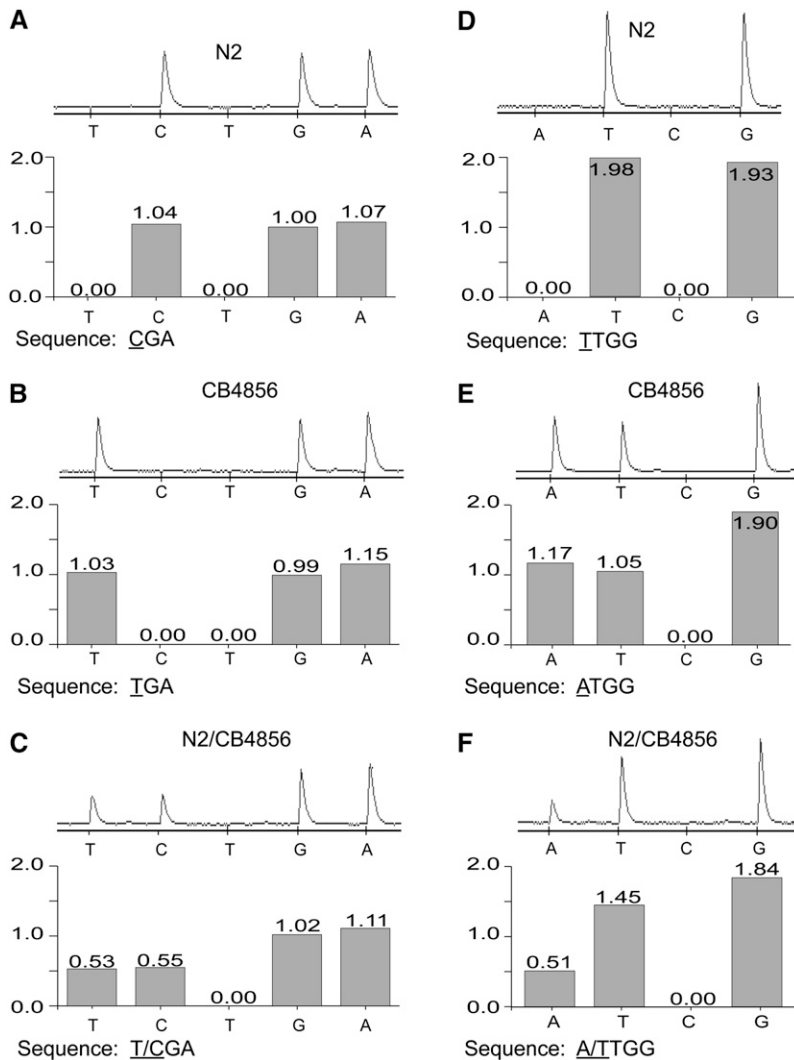


FIGURE 3.—DNA pyrosequencing is a quantitative method for genotyping *C. elegans* SNPs. (Top, A–F) Representative pyrograms depicting the analysis of DNA from N2 homozygotes (A and D), CB4856 homozygotes (B and E), and N2/CB4856 heterozygotes (C and F). The nucleotides listed below the pyrograms were added to the reaction sequentially, and the height of a peak indicates the amount of light emitted, which is proportional to the number of nucleotides incorporated into DNA. The polymorphic nucleotides are underlined (Bottom, A–F) Histograms in which the pyrogram peak heights were normalized by setting the average signal for incorporation of a single nucleotide equal to 1.0 [the values for dATP incorporation were not included in this calculation, since dATP can act as a substrate for luciferase and might contribute some false-positive signal (RONAGHI 2001)]. (A–C) The analysis of polymorphism *pkP6155*: the N2 sequence is CGA, the CB4856 sequence is TGA, and the N2/CB4856 heterozygote sequence is (C/T)GA. (D–F) The analysis of polymorphism *pkP1057*: the N2 sequence is TTGG, the CB4856 sequence is ATGG, and the N2/CB4856 heterozygote sequence is (A/T)TGG.

highly sensitive to supplemental dietary zinc, it is possible that animals containing specific combinations of N2 and CB4856 DNA might display enhanced resistance to supplemental zinc.

To determine linkage between the 19 mutations that cause zinc resistance and SNP markers, we mated males homozygous for a mutation that causes zinc resistance to CB4856 hermaphrodites and selected outcrossed, heterozygous F<sub>1</sub> hermaphrodites. F<sub>2</sub> self-progeny that are likely to be homozygous for the mutation that causes zinc resistance were identified by assaying for viability when cultured on NAMM with 0.3 mM supplemental zinc. Viable animals were allowed to self-fertilize for several generations to generate a population that is homozygous at most loci. These animals are homozygous for the mutation that causes zinc resistance and therefore homozygous for N2 DNA at this position in the genome. At positions in the genome linked in *cis* to a mutation that causes zinc resistance, these animals have a high probability of having N2 DNA. At positions in the genome unlinked to a mutation that causes zinc resistance,

such as other chromosomes, these animals have a 50% probability of having CB4856 DNA and a 50% probability of having N2 DNA. We isolated 20–48 strains that were independently derived and homozygous for the zinc-resistance mutation for each of the 19 mutations.

To determine the genotype of these strains, we prepared DNA from each strain and analyzed SNP markers at the center of each chromosome. Each strain was analyzed separately and categorized as homozygous for N2 DNA, homozygous for CB4856 DNA, or heterozygous. The results for each mutation were determined by combining the results from each strain and calculating the percentage of N2 DNA. In general, each of the 19 mutants showed a high percentage of N2 DNA at the center of one chromosome and ~50% N2 DNA at the centers of the other five chromosomes (Table 2). For example, *am129* mutants displayed 98% N2 DNA at the center marker on chromosome V and 41–66% N2 DNA at the center markers of chromosomes I, II, III, IV, and X (Table 2, line 11). In some cases, a mutation displayed moderately high linkage to two chromosomes. For

**TABLE 1**  
**Polymorphisms detected by pyrosequencing**

Polymorphism <sup>a</sup>	Location <sup>b</sup>	Clone <sup>c</sup>	Primer sequence <sup>d</sup> (5' → 3')	Substitution <sup>e</sup>	
<i>pkP1050</i> (v124d02)	I	-19.3	F56C11	*AAT GCA TGA GGG ATG GAG AA GGT GCG AAT ATG AAA AAC TCG CCA GAT CAT CAA TTT A	T → A
<i>pkP1103</i> (yw13d04)	I	-12.5	Y71G12A	*TAA GAA TGG GCA GGC ACG TA TGC CGA AAA AAA TCG TTT GC CCG CCC ACC CCT AGA	A → G
<i>pkP1105</i> (yw99b08)	I	-8.0	F32B5	*GAG GAG CAT CTG GAA CAG AAG TT TGT GTG AGT CGC AAA CTC G CGC AGT TTT TCA ATT TGT	G → C
<i>amP108</i> (yx25g02)	I	-5.2	Y54E10BL	AGG TAC CGG GAA GAA GGT CG *CGC ATT GTC GAT CTG ACC A CAT CGG CAG AGC CAG	A → G
<i>pkP1057</i> (eam67h04)	I	+1.0	K04F10	CTC GTG GTC TTC TGG CTT GAT T *ATT TCA GGA AAG CCG ACT GG CCA TAC TGA TCA CGT CAT	T → A
<i>amP109</i> (yy55h07)	I	+5.1	F59C6	*GGG TCT TCT TCA AAA TGA CAT AGG GAG TGG GTA CAT CGT TTA CTT CAT AGT CTT TCA ACT TAA TCC C	C → T
<i>amP23</i> <i>snp_F49B2[1]</i> (vc88a06)	I	+24.3	F49B2	*TCG TAG TTT GCA CTC CCT CTC GAA GAG CAA TAA GGG GCA AA TGC CCA AGA CGT AAA	T → A
<i>pkP2133</i> (eam57g09)	II	-15.6	W07E6	TGT TCG ACA AAA AGC ACA CAC *TTT CGA ACA AAT TTT CAG ATC A ATT CGT CAT ATA TTT TTT CT	T → C
<i>amP110</i> (vd51f09)	II	-2.0	C34F11	GTT CAA TAG CCT TGA TGA ATG G *AGC ACC GAT TTC AGT GAT GAT TTC AAT AAA CTT TTA ATG TT	T → C
<i>pkP2148</i> (yw08d02)	II	+0.1	C44B7	CGT GTA AAT GCT CAC CTC TGA CTC *CAA CCC CAC TTC TTC AAA GTC TT AGT TGT TGG CGA CAG	A → G
<i>pkP2110</i> (vr92g06)	II	+3.3	F37H8	*TTT ATT AAT GGA GCC CCA GGT TTG TAT CAA AAG ATC GTA GTG AAA CAA AAG ATC GTA GTG AAA AA	A → G
<i>amP111</i> <i>snp_Y54E2[2]</i> (eam54a12)	II	+23.5	Y54E2A	CGA ACA AGC CTA CAA GAC CA *TTG GGG CGA TGT AGA TGA TT CCA CGA GCA TCA AAA T	T → G
<i>amP112</i> <i>snp_H10E21[1]</i> (vm24h04)	III	-27.2	H10E21	*GAG GAG GTA CCG TAG CCA AA CGA CTT TAC GAT TCG GTT GG CGA TAA TTC AGA GCA TCA	G → A
<i>amP113</i> (vr79g08)	III	-9.0	H06I04	AGC CGC GCA ATT TTA ATG *GCC TAC CGT ATA ACC TGC ACT T CGC CCC ACC GCA CTA	C → G
<i>pkP3097</i> (yy49a05)	III	-3.9	C30D11	AAG GCA AGT ATC CCA CTG GA *GCC GTG TTA TAT TCA GCG ACA A CAA GTA TCC CAC TGG AG	T → C
<i>pkP3051</i> (vr92h05)	III	+0.6	ZK1098	AGA TGC AGG AGC AAA TTA CGA *TGG AAT CTA GGG CAC TCT TTT T CAT GAG GAG GAG ATT AAG AC	G → T
<i>pkP3073</i> (v121e06)	III	+7.1	Y47D3A	CGG TTT GCC GGA TAT TTT TAT T *TTT TTT TGG GGG CTT CAA CA CAA AGC TTC TGA CTG AAT A	G → A
<i>amP113</i> <i>snp_T28A8[1]</i> (vr79c12)	III	+21.3	T28A8	ACG GAT TCG AGT GAT GTT CG *CAG TGG ATT CCT TCC AAT GAT GTC GAA TGA CTT TTT AGA AC	A → T

(continued)

**TABLE 1**  
(Continued)

Polymorphism <sup>a</sup>	Location <sup>b</sup>	Clone <sup>c</sup>	Primer sequence <sup>d</sup> (5' → 3')	Substitution <sup>e</sup>	
<i>pkP4053</i> (yx31d07)	IV	-14.1	F52C12	GCT GAA TCA TCA AGT GAA ACT AGC *CGT CAT CGT ATC CCT TTT TGA AT AGT GAA ACT AGC TCA ATA AC	C → G
<i>amP114</i> (v130h05)	IV	-3.7	C09G12	TAG GCT TGG CCG AAT CAC *AGT AGA GCG CAT TTG CAT GA GGC CCG GCA TGT GGT	C → T
<i>pkP4064</i> (yy61a12)	IV	+0.1	F15E6	TGG AGC ATG TCA ATT CTG AAA *TTT TTA CTC GAC TGC AAT GTT TTT AAA CGG GTT TCA TAC TG	T → C
<i>dbP4</i> (eam58e05)	IV	+4.6	F01G10	AAT CAG CAT CTG CCG ATC GTT *GCA CTT GCT CAT GGC TCA GA GGG ACA CGC TTG CCC	T → A
<i>pkP4091</i> (yw97a11)	IV	+10.9	Y45F10D	ACG ATG CAT TCC ATA TTT TTA CAC *TCA ACA TTT CGA ACA CTC CTA ATC CAT AAC ATA AGT TCT ACG CA	A → G
<i>pkP4102</i> (yx31d07)	IV	+16.7	T02D1	ACC CGG ATG TCT GTC AGT CT *TTT GCG TCG AAA TTC AAA AA TCG GTC ATT TTC CAA	C → T
<i>amP56</i> <i>snp_F33E11[1]</i> (eam59c02)	V	-20.0	F33E11	*CCA ACA TTC TTG CAT GCC TA GTG CTC GAT GAA GCG AAT TT TTC CTT GCT ATG TGA CTC T	C → T
<i>pkP5092</i> (vr79c12)	V	-5.2	T28F12	GGG TCA TTG ATG AGG GGT TA *TTG CAA AAA CCT TGA ATA CGT G GAT TTT GCG ATT TTC TGA	G → A
<i>pkP5109</i> (vr91f11)	V	-2.4	C25A10	GCC ATT TCA CAT TTT GGA TAA TCA *TCG GTT CCA TGG GAA AAG TA TCA ATC TTG AAA TAT CTT CC	C → T
<i>pkP5513</i> (vr92c03)	V	+0.1	F44C4	GCC AGA TAG TGA CGA TTG TTG A *GGA AGA AGG GAA TTT GAA ATA A CAC TGG ACT ATC GTC GA	A → C
<i>oxP2/pkP5066</i> (vd50f02)	V	+3.0	T19B10	TCA AAG CTA CAG AAA ACC ACA CA *AGC ACG ACA CTT TGC ATC TG CAC AGA GAA AAT TAG GTG C	T → C
<i>pkP5123</i> (vc89g12)	V	+5.3	Y2H9A	*TTC CCT CGT AAA ACA ATT GAG AA CAA TGT TCG AAA CGC ACA AC ACA ACT CAC GAA ATT AGT AT	G → A
<i>pkP5084</i> (yw17g02)	V	+6.9	C48G7	*TCC ATG AAC CAT GTT GAA GC CTC CTG GTG GGA ATA GCT CA TGA ATA AAA TAT CTA CAT GA	T → G
<i>amP50</i> (v130h01)	V	+25.0	ZC15	AAA TTG CAC TTT GGG GGA TT *GGG CGA TGA TGA ACA GAG AG TTT TCT TCA TTC TTT CCA	C → T
<i>pkP6140</i> (vr78d03)	X	-19.5	F02G3	*GGG TTT GTT CTC GCA TTT G TAC GGG TGC CGA CAA GAA T GCA CAA GAA TTG TCC AG	C → T
<i>amP116</i> <i>snp_C31H2[3]</i> (yx32f08)	X	-6.2	C31H2	*GCG AGC AAA AAA AAA ACG ATT TA ATA AGC GTT TGC GTC TAG CTT T CCG TCG TCT TGA CAC	G → A
<i>pkP6152</i> (yy60g01)	X	-3.9	F22F4	GGA CAT AAC GTT GTC AAA AAG AA *AAT CAT TTC CTG TTT CGA ATC TG TGT TAA AGA GGA ATG TAC G	G → A
<i>pkP6155</i> (yy46g03)	X	-1.9	B0403	*TTG GCA GTC AAG AAT GTG TGG ATC GTT GCC TGG GCT TCA AAC ATG CCA GCT CCA	C → T

(continued)

**TABLE 1**  
(Continued)

Polymorphism <sup>a</sup>	Location <sup>b</sup>		Clone <sup>c</sup>	Primer sequence <sup>d</sup> (5' → 3')	Substitution <sup>e</sup>
<i>amP117</i> CE6-213 (yw98c10)	X	+1.4	F49E2	*GCA TAG ATT CAA CTA TTG CCC AAA TTT TTC GAT GTT TCG CAC AG TGC ACT TAG CCG GA	G → A
<i>pkP6160</i> (eam50a10)	X	+2.5	T05A10	GAT GAT CTC CTG CTG TAG CTC AGT *TCT CAT TGA CCG TGT ATG TGT TC GCT GAG TGA TCG TTG ATT	T → C
<i>pkP6130</i> (eam6605)	X	+7.0	B0198	AAG TGC TTG CCG GAG TAG AGG *CGA AAC AAA CCT GGG TGA CG TGT CTC CAC GCG AAT	C → T
<i>pkP6171</i> (yw11h06)	X	+24.4	C16H3	*CGA TGC GGT TTC CTA GCT TA CAT ATG GTC GCA AGA ACA GC CCA TCA TCT GAT ACA T	G → A

<sup>a</sup>In accordance with the standardized *C. elegans* nomenclature, the DNA sequence of the N2 strain is defined as wild type, and a sequence difference in the CB4856 strain was assigned an allele name. This name is composed of a two-letter laboratory designation, a "P" indicating a sequence polymorphism that does not cause a visible phenotype, and a number. Alleles that were verified in this study were given the *am* laboratory designation, with the temporarily assigned name in parentheses. Additional information about the alleles can be found on WormBase (<http://wormbase.org/>). The names in parentheses refer to the CB4856 sequence read conducted by the Genome Sequencing Center (<http://genomeold.wustl.edu/>) that was used to identify the SNP.

<sup>b</sup>Location refers to the linkage group and the interpolated genetic position of the SNP.

<sup>c</sup>Clone refers to the name of the cosmid or YAC that contains the cloned *C. elegans* DNA, including the SNP.

<sup>d</sup>For each SNP, the first two oligonucleotide primers listed were used for the initial PCR, and the third primer was used for the sequencing reaction. The primer identified with the asterisk contains the 23-nucleotide Biotin Label Sequence at its 5'-end (AGC GCT GCT CCG GTT CAT AGA TT).

<sup>e</sup>Substitution, N2 → CB4856 DNA sequence.

example, *am135* mutants displayed 77% N2 DNA at the center markers of chromosomes I and V (Table 2, line 6). This suggests that the mutation is weakly linked to the center of one of these chromosomes and unlinked

to the other chromosomes, which probably displayed a higher-than-average fraction of N2 DNA as a result of statistical fluctuations. To determine the true chromosomal linkage of *am135*, we analyzed additional markers

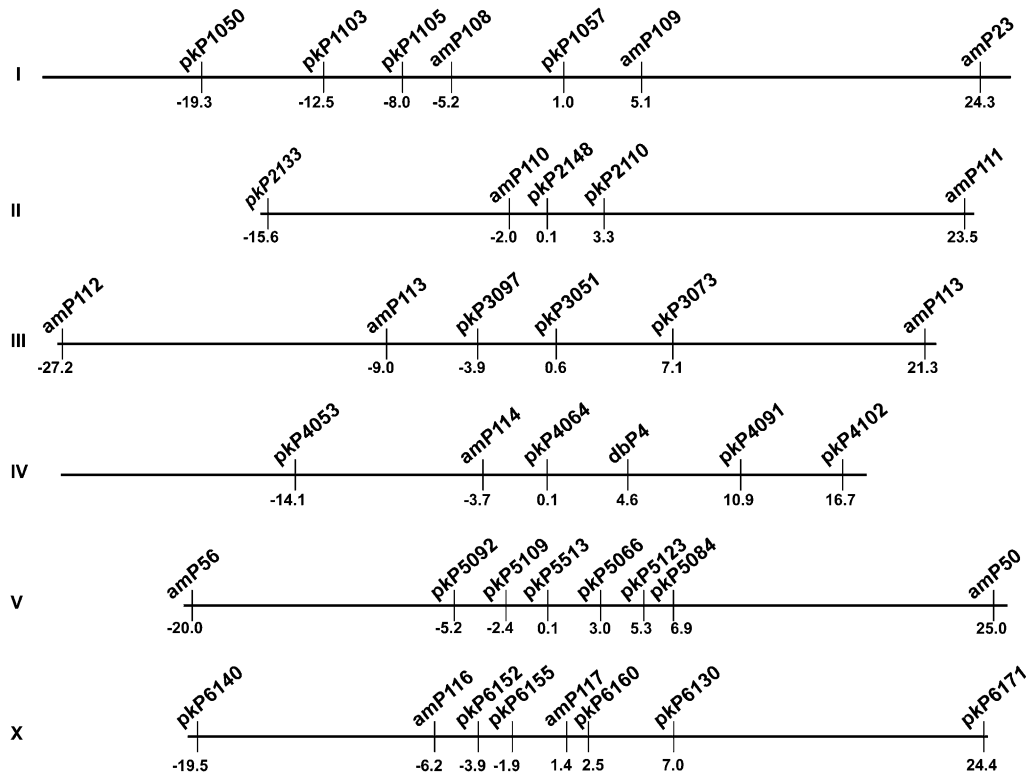


**FIGURE 4.**—Genetic map of SNP markers that can be scored by pyrosequencing. Horizontal lines represent the six chromosomes (numbered at the left), which are aligned at genetic map position 0, approximately the center. Polymorphisms between the N2 strain and the CB4856 strain are named above using the standard *C. elegans* nomenclature (two-letter laboratory designation, P for polymorphism, and a number); the position in map units is shown below. Each polymorphism is described in Table 1.

TABLE 2

Mapping mutations that cause zinc resistance using SNP markers scored by pyrosequencing in the center of each chromosome

Allele	% recombinant chromosomes with N2 genotype <sup>a</sup>					
	<i>pkP1057</i> (I) <sup>b</sup> (+1.0)	<i>pkP2148</i> (II) (+0.1)	<i>pkP3051</i> (III) (+0.6)	<i>pkP4064</i> (IV) (+0.1)	<i>pkP5513</i> (V) (+0.1)	<i>amP117</i> (X) (+1.4)
<i>am118</i>	<b>79</b>	55	71	73	71	68
<i>am120</i>	<b>83</b>	38	71	73	63	51
<i>am122</i>	<b>71</b>	39	53	68	<u>71</u>	64
<i>am124</i>	<b>87</b>	ND	74	41	57	80
<i>am125</i>	<b>76</b>	38	74	56	68	<u>76</u>
<i>am135</i>	<b>77</b>	42	68	42	<u>77</u>	63
<i>am139</i>	<b>63</b>	43	50	55	50	<u>70</u>
<i>am140</i>	<b>87</b>	46	40	68	72	63
<i>am123</i>	70	58	70	67	<b>83</b>	76
<i>am126</i>	52	57	59	67	<b>83</b>	63
<i>am129</i>	66	42	41	46	<b>98</b>	57
<i>am134</i>	62	38	46	46	<b>84</b>	42
<i>am137</i>	74	32	56	54	<b>86</b>	66
<i>am138</i>	60	29	75	59	<b>97</b>	56
<i>am128</i>	61	52	48	41	71	<b>81</b>
<i>am130</i>	73	48	52	53	50	<b>91</b>
<i>am132</i>	61	69	48	58	59	<b>95</b>
<i>am133</i>	48	33	67	48	57	<b>80</b>
<i>am136</i>	70	48	68	58	82	<b>93</b>

ND, not determined.

<sup>a</sup>Values in boldface represent true chromosomal linkage, confirmed by subsequent studies. Values underlined represent the highest fraction of N2 DNA among these six markers. A minimum of 40 recombinant chromosomes were examined at each SNP for each mutation that causes zinc resistance (see MATERIALS AND METHODS for details).

<sup>b</sup>See Table 1 for a description of the SNPs.

on both chromosomes. Mutants containing *am135* displayed 95% N2 DNA at a marker on the left arm of chromosome I, whereas no marker on chromosome V displayed >77% N2 DNA (Table 3, lines 6 and 16). These results indicate that *am135* is positioned on chromosome I. This approach was used to analyze all 19 mutations, and the results indicate that 8 mutations are positioned on chromosome I, 6 mutations are positioned on chromosome V, and 5 mutations are positioned on chromosome X (Table 2).

To determine the approximate position of each mutation on the chromosome, we analyzed additional SNP markers. For the eight mutations on chromosome I, we analyzed five additional SNP markers ranging from genetic position  $-19.3$  to  $+24.3$  (Table 3). Six mutations displayed tightest linkage to the SNP marker at  $-8.0$ , and two mutations displayed tightest linkage to the SNP marker at  $-12.5$  (Figure 5). One interpretation of these results is that all eight mutations on chromosome I affect a single gene positioned close to  $-12.5$  and  $-8.0$ . Another possible interpretation is that two mutations affect one or two genes positioned close to  $-12.5$  and six mutations affect one or more genes positioned close to  $-8.0$ . For the six mutations on chromosome V, we analyzed four additional SNP markers ranging from genetic position  $-20.0$  to  $+5.3$  (Table 3). Two mutations

displayed tightest linkage to the SNP marker at position  $-5.2$ , and four mutations displayed very tight linkage to the SNP marker at position  $+0.1$  (Figure 5). For the five mutations on chromosome X, we analyzed four additional SNP markers ranging from genetic position  $-3.9$  to  $+7.0$  (Table 3). Three mutations displayed very tight linkage to the SNP marker at position  $-3.9$ , and two mutations displayed tightest linkage to the SNP marker at position  $+2.5$  (Figure 5). While the data indicate which SNP is closest to a mutation, the data do not establish whether the mutation is positioned to the right or left of any SNP, and therefore these results cannot be used to define an interval that contains a mutation.

The mapping experiments demonstrate that the 19 zinc-resistant mutations are positioned on three different chromosomes. Therefore, these mutations affect at least 3 different genes, and they might affect as many as 19 different genes. To investigate the number of genes affected by these mutations, we attempted to perform complementation tests using mutations positioned on the same chromosome. However, all of the mutations that were analyzed were semidominant, since heterozygous animals displayed significantly greater resistance to supplemental dietary zinc than wild-type animals. Because of this semidominance, it was not possible to interpret the phenotype of *trans*-heterozygous animals

**TABLE 3**  
**Mapping mutations that cause zinc resistance to an approximate position on the chromosome using SNP markers scored by pyrosequencing**

Allele	% recombinant chromosomes with N2 genotype <sup>a</sup>					
	<i>pkP1050</i> <sup>b</sup> (-19.3)	<i>pkP1103</i> (-12.5)	<i>pkP1105</i> (-8.0)	<i>pkP1057</i> (+1.0)	<i>amP109</i> (+5.1)	<i>amP23</i> (+24.3)
	Chromosome I					
<i>am118</i>	78	<u>100</u>	89	79	ND	50
<i>am120</i>	ND	ND	<u>94</u>	83	73	ND
<i>am122</i> <sup>c</sup>	ND	77	<u>87</u>	71	ND	45
<i>am124</i>	ND	ND	<u>98</u>	87	ND	ND
<i>am125</i>	75	81	<u>100</u>	76	ND	50
<i>am135</i> <sup>c</sup>	77	89	<u>95</u>	77	74	ND
<i>am139</i> <sup>d</sup>	83	<u>98</u>	83	63	ND	45
<i>am140</i>	ND	89	<u>95</u>	87	84	ND
	% recombinant chromosomes with N2 genotype <sup>a</sup>					
Allele	<i>amP56</i> (-20.0)	<i>pkP5092</i> (-5.2)	<i>pkP5513</i> (+0.1)	<i>pkP5066</i> (+3.0)	<i>pkP5123</i> (+5.3)	
	Chromosome V					
<i>am123</i>	ND	<u>86</u>	83	ND	77	
<i>am126</i>	ND	76	<u>83</u>	76	76	
<i>am129</i>	ND	97	<u>98</u>	97	ND	
<i>am134</i>	60	72	84	<u>85</u>	84	
<i>am137</i>	83	<u>90</u>	86	ND	89	
<i>am138</i>	61	86	<u>97</u>	95	91	
<i>am122</i> <sup>c</sup>	ND	71	71	74	ND	
<i>am135</i> <sup>c</sup>	ND	63	77	73	76	
	% recombinant chromosomes with N2 genotype <sup>a</sup>					
Allele	<i>pkP6152</i> (-3.9)	<i>pkP6155</i> (-1.9)	<i>amP117</i> (+1.4)	<i>pkP6160</i> (+2.5)	<i>pkP6130</i> (+7.0)	
	Chromosome X					
<i>am128</i>	<u>85</u>	<u>85</u>	81	ND	71	
<i>am130</i>	90	ND	91	<u>93</u>	90	
<i>am132</i>	94	ND	95	<u>98</u>	95	
<i>am133</i>	<u>88</u>	ND	80	83	ND	
<i>am136</i>	<u>98</u>	<u>98</u>	93	83	78	

ND, not determined.

<sup>a</sup> Percentages were calculated from 20 to 49 independently derived mutant strains. Values underlined represent the highest fraction of N2 DNA.

<sup>b</sup> See Table 1 for a description of the SNPs.

<sup>c</sup> *am122* and *am135* showed moderately high linkage to SNP markers at the centers of chromosomes I and V (Table 2). Therefore, we analyzed additional markers on both chromosomes. Both mutations displayed highest linkage to markers on chromosome I.

<sup>d</sup> *am139* showed moderately high linkage to the markers at the center of chromosomes I and X (Table 2). Therefore, we analyzed additional markers on both chromosomes: *am139* displayed highest linkage to markers on chromosome I and was not tightly linked to markers on chromosome X (data not shown).

and use this approach to determine the number of complementation groups represented by the mutations on chromosomes I, V, and X.

**Defining intervals on the genetic map that contain mutations that cause zinc resistance by three-factor mapping using visible markers:** To confirm and refine the map positions of mutations that were determined by linkage to SNP markers, we used the independent approach of defining intervals that contain the mutations by conducting three-factor mapping experiments with mutations that cause visible phenotypes (BRENNER 1974). An

obstacle to using this approach was our observation that some mutations that cause visible phenotypes also influence the phenotype of resistance to supplemental zinc, which made it difficult to score the zinc-resistance phenotype in recombinant animals (data not shown). However, in most cases we were able to identify one or more mutations that cause a visible phenotype and did not significantly affect the zinc-resistance phenotype.

We selected representative mutations positioned on chromosomes I, V, and X to perform these studies. For the *am120* mutation on chromosome I, we performed



**TABLE 4**  
**Genotyping pooled vs. individual mutants by pyrosequencing**

Methods of analysis <sup>a</sup>	% with N2 genotype					
	<i>pkP1057</i> (I) <sup>b</sup>	<i>pkP2148</i> (II)	<i>pkP3051</i> (III)	<i>pkP4064</i> (IV)	<i>pkP5513</i> (V)	<i>amP117</i> (X)
Individual recombinants	66	42	41	46	<b>98</b>	57
Pooled (worm)	76	29	49	49	<u>94</u>	61
Pooled (DNA)	72	43	46	51	<u>93</u>	52

Values in boldface represent true chromosomal linkage, confirmed by subsequent studies. Values underlined represent the highest fraction of N2 DNA among these six markers.

<sup>a</sup> *am129/CB4856* heterozygotes were used to derive 30 rehomozygosed mutants. These 30 strains were analyzed individually, and the fraction of N2 chromosomes was calculated (line 1). Two animals from each strain were combined, and DNA was prepared from these 60 pooled worms (line 2). An aliquot of DNA from each of the 30 strains was combined, and the pooled DNA was analyzed (line 3). The values for the pooled samples are the average of two to three pyrosequencing reactions.

<sup>b</sup> See Table 1 for a description of the SNPs.

calculating the percentage of chromosomes that had N2 DNA (Table 2).

Pyrosequencing is a quantitative technique that can determine the ratio of the two polymorphic nucleotides in a DNA sample, and it has the sensitivity to detect as little as 5% of one allele (FAKHRAI-RAD *et al.* 2002). We reasoned that the analysis of recombinant, homozygous mutant strains could be accelerated by analyzing pooled samples that contain an equivalent amount of DNA from each of the mutant strains. The fraction of N2 DNA in a pooled sample should be similar to the fraction of N2 DNA calculated by analyzing each recombinant, homozygous mutant strain individually. To assess the feasibility of this approach with *C. elegans* samples, we investigated two methods of pooling the 30 recombinant, homozygous mutant strains containing the *am129* mutation. In the first method, we pooled two worms from each of the 30 homozygous mutant strains and prepared DNA from this group of 60 animals. In the second method, we isolated DNA from each of the 30 strains and pooled an approximately equal amount of each DNA sample. The pooled samples were analyzed by performing a pyrosequencing reaction with each of the six SNP markers positioned at the center of each chromosome. These reactions were repeated two or three times, and an average value was calculated. Table 4 shows that the fraction of N2 DNA determined by analyzing pooled worms and pooled DNA is similar to the fraction of N2 DNA determined by analyzing each homozygous mutant strain separately; for the *am129* mutation, both methods lead to the conclusion that the highest linkage is to chromosome V. Using this approach, it was possible to determine the chromosomal linkage of *am129* by performing 12–18 pyrosequencing reactions instead of 180.

## DISCUSSION

### The identification and characterization of mutations that cause resistance to high levels of dietary zinc: Zinc

metabolism is a fundamental process that has yet to be fully characterized. A comprehensive understanding of this process will require the identification of proteins that mediate the movement of zinc through cells and animals and the characterization of regulatory mechanisms that are used to respond to zinc deficiency and excess. Here we describe the use of a forward genetic screen to identify genes that play a role in zinc metabolism in *C. elegans*. This is a relatively unbiased approach that can identify new genes involved in this process, since the mutations were generated by random chemical mutagenesis and the phenotype that was analyzed is directly relevant to zinc metabolism. The mechanisms that cause excess zinc to be toxic and the endogenous processes that influence this toxicity are not well characterized. The mutant worms described here are resistant to toxicity caused by excess dietary zinc, indicating that the characterization of the affected genes may illuminate how cells and organisms detoxify excess zinc. Zinc toxicity is important for human health, since it is implicated in ischemic brain injury, a prevalent clinical syndrome (FREDERICKSON *et al.* 2004). Zinc that is released from dying neurons is postulated to diffuse away from the site of acute ischemic injury and damage neighboring cells, resulting in widespread cell death. Information derived from analyzing these mutations may contribute to the development of strategies for limiting the damage caused by excess zinc during processes such as ischemic injury.

Genes that can promote resistance to high levels of exogenous zinc have been identified in vertebrate cultured cells. Vertebrate cultured cells display toxicity when cultured in high levels of exogenous zinc. PALMITER and FINDLEY (1995) showed that overexpression of the ZnT1 protein in cultured vertebrate cells promotes resistance to zinc toxicity. Since ZnT1 protein is localized to the plasma membrane and promotes zinc excretion, overexpression of ZnT1 probably promotes resistance to excess zinc by reducing the cytosolic concentration of

zinc. While genetic changes that promote resistance of isolated cells to excess zinc have been described, genetic changes that cause intact animals to be resistant to exogenous zinc have not been previously reported.

We have identified mutations that increase the ability of intact *C. elegans* to resist the toxicity caused by high levels of dietary zinc. Here we consider two basic models for the mechanism of action of these mutations. The first model is that the mutations alter zinc metabolism so that the mutant animals have lower levels of internal zinc than wild-type animals. Lower levels of internal zinc could be caused by a reduction in zinc uptake or an increase in zinc excretion. For example, a reduction in the activity of ZIP proteins that uptake zinc in the gut might result in reduced zinc intake, whereas an increase in the activity of CDF proteins that excrete zinc might result in increased zinc excretion. In both examples, the mutant worms would be expected to have a lower level of internal zinc than wild-type worms, and this difference would be predicted to result in increased resistance to excess dietary zinc. However, the chromosomal positions of the mutations that cause zinc resistance do not correspond with the chromosomal positions of *C. elegans* genes encoding predicted ZIP and CDF proteins, suggesting that these mutations do not affect these protein families. The second model is that these mutants have the same levels of internal zinc as wild-type animals, but the mutations result in an increased capacity to tolerate zinc. Mechanisms that might enhance tolerance include increased zinc storage or detoxification. For example, increased activity of zinc-binding proteins such as metallothioneins might promote zinc tolerance. Furthermore, there might be metabolic processes that are inhibited by excess zinc or become deleterious in the presence of excess zinc, and the mutations might cause compensatory changes in these processes. Future experimental work will focus on testing these models. The first model predicts that the mutant animals will have reduced levels of internal zinc compared to wild-type animals, whereas the second model predicts that mutant and wild-type animals will have similar levels of zinc. To test these predictions, we are developing methods to measure the zinc content of *C. elegans*. The molecular identification of the affected genes is likely to provide important information about the mechanisms of zinc tolerance, and we are using positional cloning approaches to identify the affected genes.

**A map of single nucleotide polymorphism markers that are scored by pyrosequencing can be used to position mutations in the *C. elegans* genome:** Determining the position of a mutation on the genetic and physical maps of *C. elegans* is a critical part of using forward genetic screens to characterize a biological process. Improvements in the procedures used to position mutations have the potential to contribute to many laboratories that use *C. elegans* as a model organism. The determination of the sequence of the *C. elegans* genome

was a turning point for the use of single nucleotide polymorphism markers for mapping experiments, because it became straightforward to identify SNP markers at known genomic positions (WICKS *et al.* 2001). Compared to mutations that cause a visible phenotype, SNP markers have three important advantages. First, SNP markers do not cause a phenotype that interferes with scoring the phenotype of interest. An important caveat is that some phenotypes that can be scored in the wild-type N2 background are difficult to score in a mixed background of N2 and a wild isolate strain that contains many SNP markers. Furthermore, genetic incompatibilities have been described between N2 and Hawaii strains that might influence mapping experiments (SEIDEL *et al.* 2008). Second, SNP markers are abundant in wild isolates of *C. elegans*, so multiple SNP markers can be scored in a single group of recombinant animals. Third, the exact location of a SNP marker on the *C. elegans* physical map is known. As a result of these advantages, SNP markers are now used routinely to position *C. elegans* mutations in the genome.

To fully exploit SNPs as mapping markers, investigators need maps of SNP markers at two scales: a low-density genomewide map that can be used to determine the approximate position of any mutation and high-density local maps that can be used to determine the precise position of a particular mutation as part of a positional cloning strategy. The creation and use of both types of maps requires two steps: the identification of SNPs and a method for scoring SNPs. We described the creation of a local, high-density SNP map that was used for fine-scale mapping of a mutation that affects *cdf-1* (JAKUBOWSKI and KORNFIELD 1999). This approach was used to position the *cdf-1(n2527)* mutation to an interval of 9.6 kb. For this experiment, DNA sequencing was used to identify and score SNPs. Because a local, high-density map is typically used only once and the experiment does not involve scoring a large number of recombinants, the use of DNA sequencing as a scoring method is feasible. By contrast, a genomewide map is used reiteratively, and the ease of scoring the SNP markers is critical. The step of identifying SNP markers for a genomewide map was addressed by WICKS *et al.* (2001) and SWAN *et al.* (2002) who used high-throughput DNA sequencing to identify >17,000 polymorphisms in the CB4856 isolate. Many of these polymorphisms are predicted to affect a restriction enzyme recognition site, and it was demonstrated that 493 polymorphisms can be scored by a restriction enzyme digest and gel electrophoresis (WICKS *et al.* 2001). DAVIS *et al.* (2005) identified a subset of these polymorphisms that affect the recognition site for the enzyme *DraI* and are well dispersed throughout the genome. These markers can be scored using one restriction enzyme, and they form a convenient set for initial mapping experiments. The limitation of these approaches is that restriction enzyme digests and gel electrophoresis are not well suited to high-

throughput analysis. SWAN *et al.* (2002) described the use of the high-throughput method of FP-TDI to score *C. elegans* SNPs, ZIPPERLEN *et al.* (2005) described the use of FLP to score small insertion/deletion polymorphisms in *C. elegans*, and SHELTON (2006) described the use of quantitative PCR to score *C. elegans* SNPs. These methods are powerful, but they require specialized equipment that may not be available. To increase the options for scoring SNPs, we identified a subset of polymorphisms identified by WICKS *et al.* (2001) that can be scored by pyrosequencing and are well dispersed in the genome (Figure 4). Here we demonstrate that these markers can be used to position newly identified mutations. We verified the accuracy of the map positions using the traditional method of mapping relative to mutations that cause a visible phenotype. Furthermore, we demonstrate that the method can be used to accurately analyze pooled samples, thus reducing significantly the number of analytic reactions that must be performed. This approach is likely to be generally useful for determining the map position of *C. elegans* mutations, and it provides a new SNP scoring option that may be available to more laboratories. Using improved techniques for high-throughput DNA sequencing, HILLIER *et al.* (2008) recently reported resequencing the whole *C. elegans* genome, raising the possibility that whole-genome sequencing could be used to identify chemically induced mutations. The combination of SNP mapping to identify a genomic region that contains a new mutation and whole-genome resequencing to identify candidate base changes in that genomic region could be a powerful approach to cloning genes.

Some strains were provided by the *Caenorhabditis* Genetics Center. This research was supported by grants from the National Institutes of Health to K.K. (GM068598, CA84271, and AG026561). K.K. was a scholar of the Leukemia and Lymphoma Society and is a Senior Scholar of the Ellison Medical Foundation.

#### LITERATURE CITED

- AHMADIAN, A., M. EHN and S. HOBER, 2006 Pyrosequencing: history, biochemistry and future. *Clin. Chim. Acta* **363**: 83–94.
- BIRD, A., M. V. EVANS-GALEA, E. BLANKMAN, H. ZHAO, H. LUO *et al.*, 2000 Mapping the DNA binding domain of the Zap1 zinc-responsive transcriptional activator. *J. Biol. Chem.* **275**: 16160–16166.
- BRENNER, S., 1974 The genetics of *Caenorhabditis elegans*. *Genetics* **77**: 71–94.
- BRUINSMA, J. J., T. JIRAKULAPORN, A. J. MUSLIN and K. KORNFELD, 2002 Zinc ions and cation diffusion facilitator proteins regulate Ras-mediated signaling. *Dev. Cell* **2**: 567–578.
- CHIMIENTI, F., S. DEVERGNAS, F. PATTOU, F. SCHUIT, R. GARCIA-CUENCA *et al.*, 2006 In vivo expression and functional characterization of the zinc transporter ZnT8 in glucose-induced insulin secretion. *J. Cell Sci.* **119**: 4199–4206.
- COLVIN, R. A., C. P. FONTAINE, M. LASKOWSKI and D. THOMAS, 2003 Zn<sup>2+</sup> transporters and Zn<sup>2+</sup> homeostasis in neurons. *Eur. J. Pharmacol.* **479**: 171–185.
- COYLE, P., J. C. PHILCOX, L. C. CAREY and A. M. ROFE, 2002 Metallothionein: the multipurpose protein. *Cell. Mol. Life Sci.* **59**: 627–647.
- DAVIS, M. W., M. HAMMARLUND, T. HARRACH, P. HULLETT, S. OLSEN *et al.*, 2005 Rapid single nucleotide polymorphism mapping in *C. elegans*. *BMC Genomics* **6**: 118.
- DE STASIO, E., C. LEPHOTO, L. AZUMA, C. HOLST, D. STANISLAUS *et al.*, 1997 Characterization of revertants of *unc-93(e1500)* in *Caenorhabditis elegans* induced by *N*-ethyl-*N*-nitrosourea. *Genetics* **147**: 597–608.
- EIDE, D. J., 2003 Multiple regulatory mechanisms maintain zinc homeostasis in *Saccharomyces cerevisiae*. *J. Nutr.* **133**: 1532S–1535S.
- EIDE, D. J., 2004 The SLC39 family of metal ion transporters. *Pflügers Arch.* **447**: 796–800.
- ENG, B. H., M. L. GUERINOT, D. EIDE and M. H. SAIER, 1998 Sequence analyses and phylogenetic characterization of the ZIP family of metal ion transport proteins. *J. Membr. Biol.* **166**: 1–7.
- FAKHRAI-RAD, H., N. POURMAND and M. RONAGHI, 2002 Pyrosequencing: an accurate detection platform for single nucleotide polymorphisms. *Hum. Mutat.* **19**: 479–485.
- FREDERICKSON, C. J., and A. I. BUSH, 2001 Synaptically released zinc: physiological functions and pathological effects. *Biometals* **14**: 353–366.
- FREDERICKSON, C. J., W. MARET and M. P. CUAJUNCO, 2004 Zinc and excitotoxic brain injury: a new model. *Neuroscientist* **10**: 18–25.
- FREEDMAN, J. H., L. W. SLICE, D. DIXON, A. FIRE and C. S. RUBIN, 1993 The novel metallothionein genes of *Caenorhabditis elegans*. *J. Biol. Chem.* **268**: 2554–2564.
- GAITHER, L. A., and D. J. EIDE, 2001 Eukaryotic zinc transporters and their regulation. *Biometals* **14**: 251–270.
- GITAN, R. S., and D. J. EIDE, 2000 Zinc-regulated ubiquitin conjugation signals endocytosis of the yeast *ZRT1* zinc transporter. *Biochem. J.* **346**: 329–336.
- GOLDSTEIN, J. L., D. GLOSSIP, S. NAYAK and K. KORNFELD, 2006 The CRAL/TRIO and GOLD domain protein CGR-1 promotes induction of vulval cell fates in *Caenorhabditis elegans* and interacts genetically with the Ras signaling pathway. *Genetics* **172**: 929–942.
- GUERINOT, M. L., 2000 The ZIP family of metal transporters. *Biochim. Biophys. Acta* **1465**: 190–198.
- HANTKE, K., 2005 Bacterial zinc uptake and regulators. *Curr. Opin. Microbiol.* **8**: 196–202.
- HILLIER, L. W., G. T. MARTH, A. R. QUINLAN, D. DOOLING, G. FEWELL *et al.*, 2008 Whole-genome sequencing and variant discovery in *C. elegans*. *Nat. Methods* **5**: 183–188.
- HUANG, L., and J. GITTSCHIER, 1997 A novel gene involved in zinc transport is deficient in the lethal milk mouse. *Nat. Genet.* **17**: 292–297.
- JAKUBOWSKI, J., and K. KORNFELD, 1999 A local, high-density, single-nucleotide polymorphism map used to clone *Caenorhabditis elegans cdf-1*. *Genetics* **153**: 743–753.
- KURY, S., B. DRENO, S. BEZIEAU, S. GIRAUDET, M. KHARFI *et al.*, 2002 Identification of SLC39A4, a gene involved in acrodermatitis enteropathica. *Nat. Genet.* **31**: 239–240.
- LANDER, E. S., L. M. LINTON, B. BIRREN, C. NUSBAUM, M. C. ZODY *et al.*, 2001 Initial sequencing and analysis of the human genome. *Nature* **409**: 860–921.
- LANGAEE, T., and M. RONAGHI, 2005 Genetic variation analyses by Pyrosequencing. *Mutat. Res.* **573**: 96–102.
- LICHTLEN, P., and W. SCHAFFNER, 2001 Putting its fingers on stressful situations: the heavy metal-regulatory transcription factor MTF-1. *BioEssays* **23**: 1010–1017.
- LIUZZI, J. P., and R. J. COUSINS, 2004 Mammalian zinc transporters. *Annu. Rev. Nutr.* **24**: 151–172.
- MARET, W., 2003 Cellular zinc and redox states converge in the metallothionein/thionein pair. *J. Nutr.* **133**: 1460S–1462S.
- MOILANEN, L. H., T. FUKUSHIGE and J. H. FREEDMAN, 1999 Regulation of metallothionein gene transcription. *J. Biol. Chem.* **274**: 29655–29665.
- PALMITER, R. D., and S. D. FINDLEY, 1995 Cloning and functional characterization of a mammalian zinc transporter that confers resistance to zinc. *EMBO J.* **14**: 639–649.
- PALMITER, R. D., and L. HUANG, 2004 Efflux and compartmentalization of zinc by members of the SLC30 family of solute carriers. *Pflügers Arch.* **447**: 744–751.
- RIDDLE, D. L., T. BLUMENTAL, B. J. MEYER and J. R. PRIEST (Editors), 1997 *C. elegans II*. Cold Spring Harbor Laboratory Press, Cold Spring Harbor, NY.
- RONAGHI, M., 2001 Pyrosequencing sheds light on DNA sequencing. *Genome Res.* **11**: 3–11.

- SAMET, J. M., B. J. DEWAR, W. WU and L. M. GRAVES, 2003 Mechanisms of Zn<sup>2+</sup>-induced signal initiation through the epidermal growth factor receptor. *Toxicol. Appl. Pharmacol.* **191**: 86–93.
- SEIDEL, H. S., M. V. ROCKMAN and L. KRUGLYAK, 2008 Widespread genetic incompatibility in *C. elegans* maintained by balancing selection. *Science* **319**: 589–594.
- SHELTON, C. A., 2006 Quantitative PCR approach to SNP detection and linkage mapping in *Caenorhabditis elegans*. *Biotechniques* **41**: 583–588.
- SLADEK, R., G. ROCHELEAU, J. RUNG, C. DINA, L. SHEN *et al.*, 2007 A genome-wide association study identifies novel risk loci for type 2 diabetes. *Nature* **445**: 881–885.
- SWAIN, S. C., K. KEUSEKOTTEN, R. BAUMEISTER and S. R. STÜRZENBAUM, 2004 *C. elegans* metallothioneins: new insights into the phenotypic effects of cadmium toxicosis. *J. Mol. Biol.* **341**: 951–959.
- SWAN, K. A., D. E. CURTIS, K. B. MCKUSICK, A. V. VOINOV, F. A. MAPA *et al.*, 2002 High-throughput gene mapping in *Caenorhabditis elegans*. *Genome Res.* **12**: 1100–1105.
- TAPIERO, H., and K. D. TEW, 2003 Trace elements in human physiology and pathology: zinc and metallothioneins. *Biomed. Pharmacother.* **57**: 399–411.
- VALLEE, B. L., and K. H. FALCHUK, 1993 The biochemical basis of zinc physiology. *Physiol. Rev.* **73**: 79–118.
- VASAK, M., 2005 Advances in metallothionein structure and functions. *J. Trace Elem. Med. Biol.* **19**: 13–17.
- VATAMANIUK, O. K., E. A. BUCHER, J. T. WARD and P. A. REA, 2001 A new pathway for heavy metal detoxification in animals. *J. Biol. Chem.* **276**: 20817–20820.
- VATAMANIUK, O. K., E. A. BUCHER, M. V. SUNDARAM and P. A. REA, 2005 CeHMT-1, a putative phytochelatin transporter, is required for cadmium tolerance in *Caenorhabditis elegans*. *J. Biol. Chem.* **280**: 23684–23690.
- WALL, M. J., 2005 A role for zinc in cerebellar synaptic transmission? *Cerebellum* **4**: 224–229.
- WANG, K., B. ZHOU, Y. M. KUO, J. ZEMANSKY and J. GITSCHER, 2002 A novel member of zinc transporter family is defective in acrodermatitis enteropathica. *Am. J. Hum. Genet.* **71**: 66–73.
- WICKS, S. R., R. T. YEH, W. R. GISH, R. H. WATERSTON and R. H. PLASTERK, 2001 Rapid gene mapping in *Caenorhabditis elegans* using a high density polymorphism map. *Nat. Genet.* **28**: 160–164.
- WILLIAMS, B. D., B. SCHRANK, C. HUYNH, R. SHOWNKEEN and R. H. WATERSTON, 1992 A genetic mapping system in *Caenorhabditis elegans* based on polymorphic sequence-tagged sites. *Genetics* **131**: 609–624.
- WU, W., L. M. GRAVES, I. JASPERS, R. B. DEVLIN, W. REED *et al.*, 1999 Activation of the EGF receptor signaling pathway in human airway epithelial cells exposed to metals. *Am. J. Physiol.* **277**: L924–L931.
- YAMASAKI, S., K. SAKATA-SOGAWA, A. HASEGAWA, T. SUZUKI, K. KABU *et al.*, 2007 Zinc is a novel intracellular second messenger. *J. Cell Biol.* **177**: 637–645.
- YANDELL, M. D., L. G. EDGAR and W. B. WOOD, 1994 Trimethylpsoralen induces small deletion mutations in *Caenorhabditis elegans*. *Proc. Natl. Acad. Sci. USA* **91**: 1381–1385.
- YODER, J. H., H. CHONG, K. GUAN and M. HAN, 2004 Modulation of KSR activity in *Caenorhabditis elegans* by Zn ions, PAR-1 kinase and PP2A phosphatase. *EMBO J.* **23**: 1–9.
- ZHAO, H., and D. J. EIDE, 1997 Zap1p, a metalloregulatory protein involved in zinc-responsive transcriptional regulation in *Saccharomyces cerevisiae*. *Mol. Cell. Biol.* **17**: 5044–5052.
- ZHAO, H., E. BUTLER, J. RODGERS, T. SPIZZO, S. DUESTERHOEFT *et al.*, 1998 Regulation of zinc homeostasis in yeast by binding of the ZAP1 transcriptional activator to zinc-responsive promoter elements. *J. Biol. Chem.* **273**: 28713–28720.
- ZIPPERLEN, P., K. NAIRZ, I. RIMANN, K. BASLER, E. HAFEN *et al.*, 2005 A universal method for automated gene mapping. *Genome Biol.* **6**: R19.

Communicating editor: D. I. GREENSTEIN